OPEN ACCESS
CellPress

Cell Reports
Article

A Role for Stargazin in Experience-Dependent Plasticity

Susana R. Louros,[1,2,3] Bryan M. Hooks,[3] Liza Litvina,[3] Ana Luisa Carvalho,[2,4,*] and Chinfei Chen[3,*]
[1]PhD Program in Experimental Biology and Biomedicine, Center for Neuroscience and Cell Biology, University of Coimbra, 3004-504 Coimbra, Portugal
[2]Center for Neuroscience and Cell Biology, University of Coimbra, 3004-504 Coimbra, Portugal
[3]F.M. Kirby Neurobiology Center, Children's Hospital, Boston, Harvard Medical School, 300 Longwood Avenue, Boston, MA 02115, USA
[4]Department of Life Sciences, University of Coimbra, 3001-401 Coimbra, Portugal
*Correspondence: alc@cnc.uc.pt (A.L.C.), chinfei.chen@childrens.harvard.edu (C.C.)
http://dx.doi.org/10.1016/j.celrep.2014.04.054

SUMMARY

During development, neurons are constantly refining their connections in response to changes in activity. Experience-dependent plasticity is a key form of synaptic plasticity, involving changes in α-amino-3-hydroxy-5-methyl-4-isoxazolepropionic acid receptor (AMPAR) accumulation at synapses. Here, we report a critical role for the AMPAR auxiliary subunit stargazin in this plasticity. We show that stargazin is functional at the retinogeniculate synapse and that in the absence of stargazin, the refinement of the retinogeniculate synapse is specifically disrupted during the experience-dependent phase. Importantly, we found that stargazin expression and phosphorylation increased with visual deprivation and led to reduced AMPAR rectification at the retinogeniculate synapse. To test whether stargazin plays a role in homeostatic plasticity, we turned to cultured neurons and found that stargazin phosphorylation is essential for synaptic scaling. Overall, our data reveal an important role for stargazin in regulating AMPAR abundance and composition at glutamatergic synapses during homeostatic and experience-dependent plasticity.

INTRODUCTION

Proper wiring of neural circuits during development depends on both molecular cues that guide connectivity and activity-dependent mechanisms that adjust the strength and number of synaptic connections. One powerful experimental system for studying these processes is the murine visual system. For example, the retinogeniculate synapse, the connection between retinal ganglion cells (RGC) and relay neurons in the dorsal lateral geniculate nucleus (LGN) of the thalamus, exhibits well characterized phases of plasticity and circuit maturation (Hong and Chen, 2011). After the initial mapping of RGC axon terminals to their target, a phase of synapse elimination and strengthening that depends on spontaneous activity, not vision, results in a rough draft of the final circuit configuration. This phase is followed by a critical period during which visual experience further refines and stabilizes the mature circuit. Visual deprivation during this later phase (postnatal day 20 [P20], late dark rearing [LDR]) results in weakening of the average RGC input and recruitment of additional afferents. In contrast, chronic dark rearing (CDR) from birth does not elicit major synaptic rearrangements (Hooks and Chen, 2006).

The mechanisms that underlie remodeling of the thalamic circuitry in response to LDR are not well understood. Hebbian processes are thought to contribute to spontaneous activity-dependent plasticity during retinogeniculate development (Butts et al., 2007; Krahe and Guido, 2011; Ziburkus et al., 2009). However, afferent innervation increases in response to LDR and, conversely, synaptic strength decreases in visually deprived mice exposed to light for the first time at P20 (Lin et al., 2014). These responses suggest that homeostatic mechanisms could play a role in experience-dependent plasticity. In response to alterations in neuronal activity, homeostatic plasticity maintains the stability of the network activity within a dynamic range for effective information transfer (Turrigiano, 2008). Importantly, manipulation of visual experience in vivo has been shown to induce homeostatic adjustments in other regions of the visual system (Chandrasekaran et al., 2005, 2007; Desai et al., 2002; Krahe and Guido, 2011; Maffei and Turrigiano, 2008). Consistent with a role for homeostatic mechanisms in experience-dependent plasticity, recent studies have demonstrated the importance of MeCP2, a transcriptional regulator associated with Rett syndrome, in synaptic scaling in vitro (Qiu et al., 2012; Zhong et al., 2012) and in the visual cortical scaling up in response to visual deprivation (Blackman et al., 2012). Studies from our own lab have demonstrated that MeCP2 plays an essential role in experience-dependent plasticity at the retinogeniculate synapse (Noutel et al., 2011). Yet, how homeostatic plasticity mediates synaptic remodeling in vivo and in vitro is still not clear.

Because α-amino-3-hydroxy-5-methyl-4-isoxazolepropionic acid receptors (AMPARs) are central to the plasticity of connections in the LGN, dynamic regulation of these receptors must be essential for experience-dependent circuit rewiring. Thus, we examined the involvement of stargazin, an auxiliary subunit of AMPARs that regulates their delivery to the synapse (Chen et al., 2000; Opazo et al., 2010). Here, we describe essential roles of STG phosphorylation in both synaptic scaling and experience-dependent plasticity.

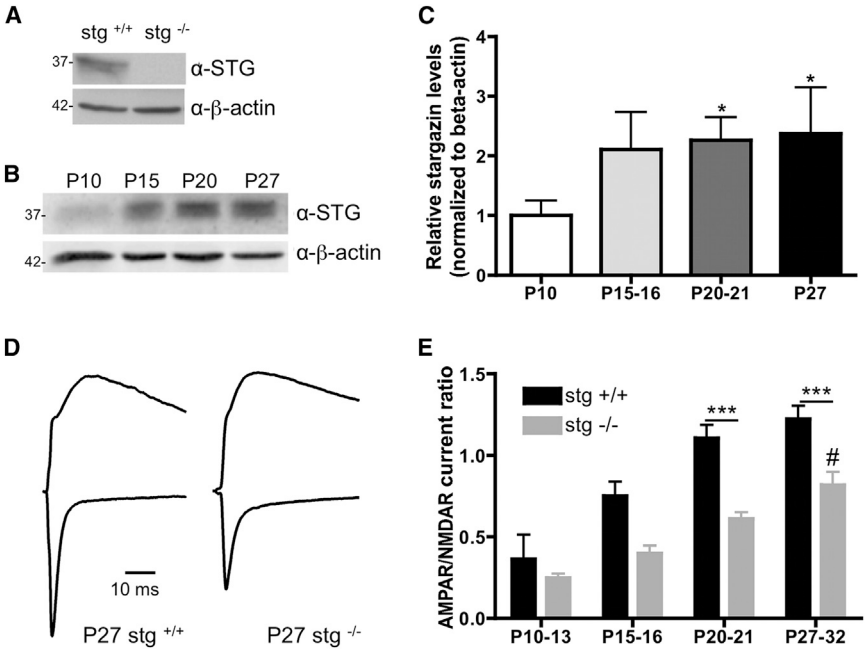

Figure 1. STG Is Important for AMPAR Trafficking in the Retinogeniculate Synapse

(A) Representative western blot from LGNs of P27 $stg^{+/+}$ and $stg^{-/-}$ mice, showing that the STG antibody used in this study is specific.

(B) Representative western blot against total STG in mouse LGNs at different developmental ages.

(C) STG levels significantly increase after eye opening and remain high up to P27 (n = 4, t test, $^{*}p < 0.05$).

(D) Representative synaptic recordings from P27 $stg^{-/-}$ and $stg^{+/+}$ mice. Superimposed glutamatergic AMPAR and NMDAR currents were evoked at HP = −70 mV (inward currents) and +40 mV (outward currents), respectively. Currents are normalized to the peak NMDAR current amplitude.

(E) Comparison of the average peak AMPAR/NMDAR current ratio over development in $stg^{-/-}$ and $stg^{+/+}$ littermates. $stg^{-/-}$ (P10–13): 13 cells from 6 animals; (P15–16): 26 cells from 9 animals; (P20–21) 23 cells from 15 animals; (P27–32): 38 cells from 23 animals. $stg^{+/+}$ (P10–13): 9 cells from 2 animals; (P15–16): 19 cells from 6 animals; (P20–21): 21 cells from 10 animals; (P27–32): 36 cells from 23 animals. ANOVA, Bonferroni test,$^{***}p < 0.001$ $stg^{-/-}$ versus WT; $\#p < 0.01$ $stg^{-/-}$ P27–32 versus $stg^{-/-}$ P15.

In (C) and (E), data are presented as mean ± SEM. See also Figure S1.

RESULTS

Stargazin Is Essential for Retinogeniculate Synapse Remodeling

Developmental remodeling at the retinogeniculate synapse is notable for the robust synapse strengthening that occurs during normal development, as well as the change in strength and connectivity that occurs in response to visual deprivation. In both cases, the regulation of AMPAR presence in the postsynaptic densities must be critical for rewiring the circuit. Many molecules have been associated with AMPAR, including the transmembrane AMPAR regulatory proteins (TARPs). The protein stargazin (STG) is one of the best-characterized proteins of this class, and thus we first asked whether this TARP plays a role in retinogeniculate synapse remodeling. To determine whether STG is expressed in the LGN, we dissected LGNs from acute mouse brain slices at different ages and looked at total STG expression by western blot. The antibody used in this study recognizes a 37 kDa band that is absent in stargazer mice that lack STG expression (Letts et al., 1998), confirming this band as STG (Figure 1A). In wild-type (WT) mice, STG protein levels in the LGN increase after P10, reaching maximal levels of expression after P15, a developmental time point just after eye opening (P12) (Figures 1B and 1C). STG expression remains elevated at P27–32, when synaptic strength has reached the mature level ($p = 0.03$, t test, P10 compared with P27).

The LGN contains two classes of neurons: (1) excitatory relay neurons that project to the visual cortex and (2) intrinsic inhibitory neurons. Although both classes of neurons receive retinal inputs, relay neurons outnumber interneurons by 4:1 (Ohara et al., 1983). To test whether STG plays a role specifically at retinogeniculate synapses, we examined the stargazer mouse. We found that the AMPAR/NMDAR current ratio was reduced at all ages in stargazer mice compared with their WT littermates, consistent with a role for STG in AMPAR insertion at the synapse (Figures 1D and 1E). The deficit is most severe in older mice (AMPAR/NMDA ratio of 1.22 versus 0.82 at P27–32, $p < 0.001$, ANOVA, Bonferroni test). Despite the lack of STG, however, the ratio increased from 0.40 to 0.82 between P15 and P32 in stargazer mice ($p < 0.01$ ANOVA, Bonferroni test). This suggests that other AMPAR-interacting proteins are also responsible for AMPAR insertion at retinogeniculate synapses (Fukaya et al., 2005; Payne, 2008). Indeed, we detected TARPγ4 expression in LGN with a developmental expression pattern similar to that of STG (Figure S1A), which may explain the persistence of synaptic AMPARs in stargazer mice (Tomita et al., 2003). However, we did not detect a change in TARPγ4 expression levels in the LGN of stargazer mice relative to WT (Figure S1B). These results clearly implicate STG in the trafficking and insertion of AMPAR at the retinogeniculate synapse.

If STG is involved in AMPAR trafficking into the retinogeniculate synapse, it could play a role in the developmental refinement of this circuit. We compared the single-fiber strength and number of afferent inputs onto relay neurons in stargazer and WT littermates. Figure 2 shows representative examples of AMPAR- and NMDAR-mediated currents from WT (Figure 2A) and stargazer (Figure 2B) littermates in response to increasing stimulus intensities at P15–16 (top) and P27–32 (bottom). Consistent with previous reports (Tomita et al., 2005; Sumioka et al., 2010), the evoked synaptic currents in $stg^{-/-}$ mice differed from those in $stg^{+/+}$ mice with regard to their AMPAR/NMDAR ratio (Figures 2A and 2B) (Lacey et al., 2012; Menuz and Nicoll,

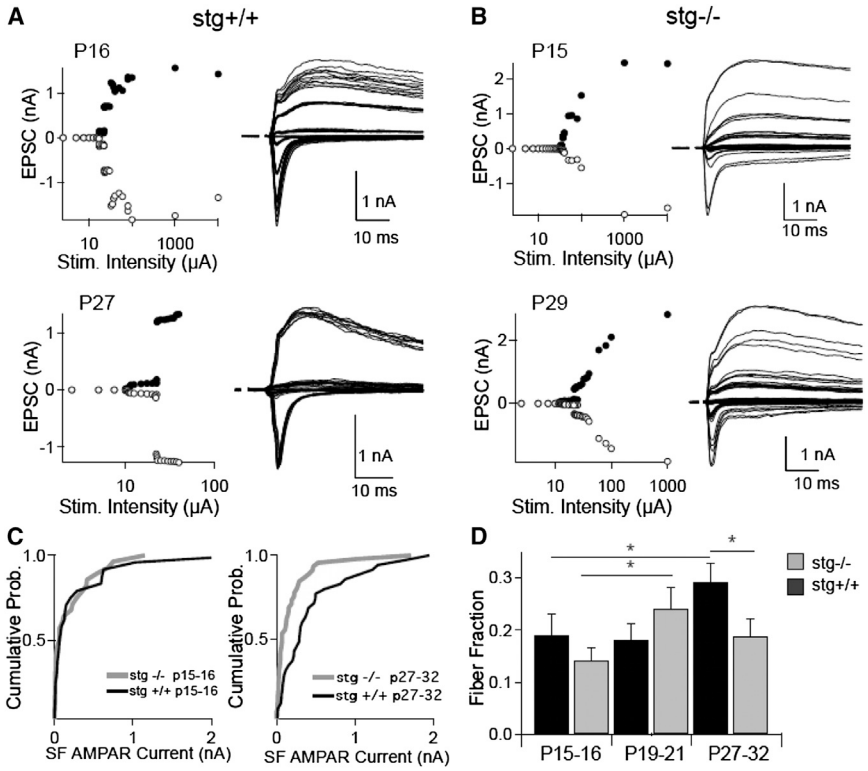

Figure 2. STG Is Important for the Late Phase of Retinogeniculate Synapse Refinement

(A and B) Representative recordings from $stg^{+/+}$ (A) and $stg^{-/-}$ (B) littermates at P15–16 (top panels) and P27–32 (lower panels). Left: plot of the peak EPSC amplitude (nA) vs. stimulus intensity for both AMPAR-mediated (white circles) and NMDAR-mediated (black circles) components of the synaptic current. Right: superimposed EPSCs recorded from the same relay neuron at −70 mV (inward currents) or +40 mV (outward currents) while the stimulus intensity was increased.

(C) Comparison of single-fiber (SF) AMPAR current amplitude cumulative probability histograms for $stg^{-/-}$ and $stg^{+/+}$ littermates during the spontaneous activity-dependent (P15–16) and experience-dependent (P27–32) phases of synaptic remodeling (n = 24–45). $stg^{-/-}$ mice were significantly different from their $stg^{+/+}$ littermates at P27–32, but not at P15–16 (Mann-Whitney).

(D) Comparison of fiber fraction over development (*$p < 0.05$, by one-way ANOVA, Kruskal-Wallis test with Dunn's multiple comparison, n = 48–93). A higher fiber fraction indicates fewer afferent inputs and a more refined circuit. Data are presented as mean ± SEM.

See also Figure S2.

2008). However, at P15–16, the average AMPAR and NMDAR single-fiber current amplitudes were similar for the two genotypes (for AMPAR, Figure 2C). To estimate the number of afferent inputs, we calculated the fiber fraction ratio, which quantifies the fractional contribution of that input to the maximum current of a given cell (Hooks and Chen, 2006). The fiber fraction ratio was not changed in the absence of STG at P15–16 (Figure 2D). Similarly, analysis of retinogeniculate connectivity at P19–21 revealed no significant differences in single-fiber strength (data not shown, Mann-Whitney test: $p = 0.1$, n = 29–31) or fiber fraction (Figure 2D). However, after the vision-dependent phase of synaptic remodeling (between P20 and P34), differences between WT and mutant mice became evident: single-fiber AMPAR excitatory postsynaptic current (EPSC) amplitudes were significantly smaller in $stg^{-/-}$ mice, as shown by the leftward shift in the cumulative probability amplitude distribution at P27–32 (Figure 2C, right; Kolmogorov-Smirnov test: $p = 0.003$). Moreover, the fiber fraction was significantly reduced in $stg^{-/-}$ mice, consistent with an increased number of afferent inputs (0.29 ± 0.04, n = 70 in WT p27–32, compared with 0.19 ± 0.03, n = 88 in $stg^{-/-}$ mice; Figure 2D). Therefore, even in the absence of STG, retinogeniculate synapses strengthen and refine during the spontaneous activity-dependent phase development (<P20). However, synaptic connectivity becomes significantly disrupted later in development, during the vision-sensitive period of the thalamic circuit.

Stargazer mice exhibit frequent absence-like seizures (Burgess and Noebels, 1999), raising the possibility that pre-P20 seizures may disrupt experience-dependent synaptic refinement. To test this possibility, we examined synaptic maturation in another mouse seizure model, the Tottering mouse. In Tottering, a mutation in the P/Q-type HVA voltage-gated calcium channel subunit α1A (Cacna1a) leads to a similar phenotype as stargazer, with onset of absence-like seizures by P15 (Burgess and Noebels, 1999). Figure S2 shows that in contrast to $stg^{-/-}$ mice, refinement in Tottering mice is normal at P27–32. Therefore, increased excitability of thalamic circuits from absence-like seizures per se does not disrupt retinogeniculate refinement. Taken together, these results point to a specific role of STG in experience-dependent synaptic remodeling.

Stargazin Expression Is Regulated by Visual Experience

To test whether STG is regulated by experience, we compared the expression levels of STG in C57BL/6J mice exposed to different visual manipulations. We have previously demonstrated that visual deprivation from birth (CDR) does not elicit changes in synaptic connectivity, whereas dark rearing for 1 week at P20 (LDR) elicits robust rearrangements of the retinogeniculate synapse, weakening single-fiber strength and increasing the number of afferent inputs (Hooks and Chen, 2006, 2008). STG levels significantly increased in the LGN of LDR, but not CDR, mice (Figures 3A and 3B; $p = 0.03$ for STG levels in LDR compared with light-reared (LR) mice, ANOVA followed by Dunnett's test). In contrast, the expression of TARPγ4 was not changed by either visual manipulation (Figures 3C and 3D, n = 3, $p = 0.63$, ANOVA), consistent with an important role for STG in the remodeling of the retinogeniculate synapse during LDR.

The function of STG is regulated by the phosphorylation of nine consecutive serine residues in the cytoplasmatic tail of the protein, and this phosphorylation regulates the interaction of

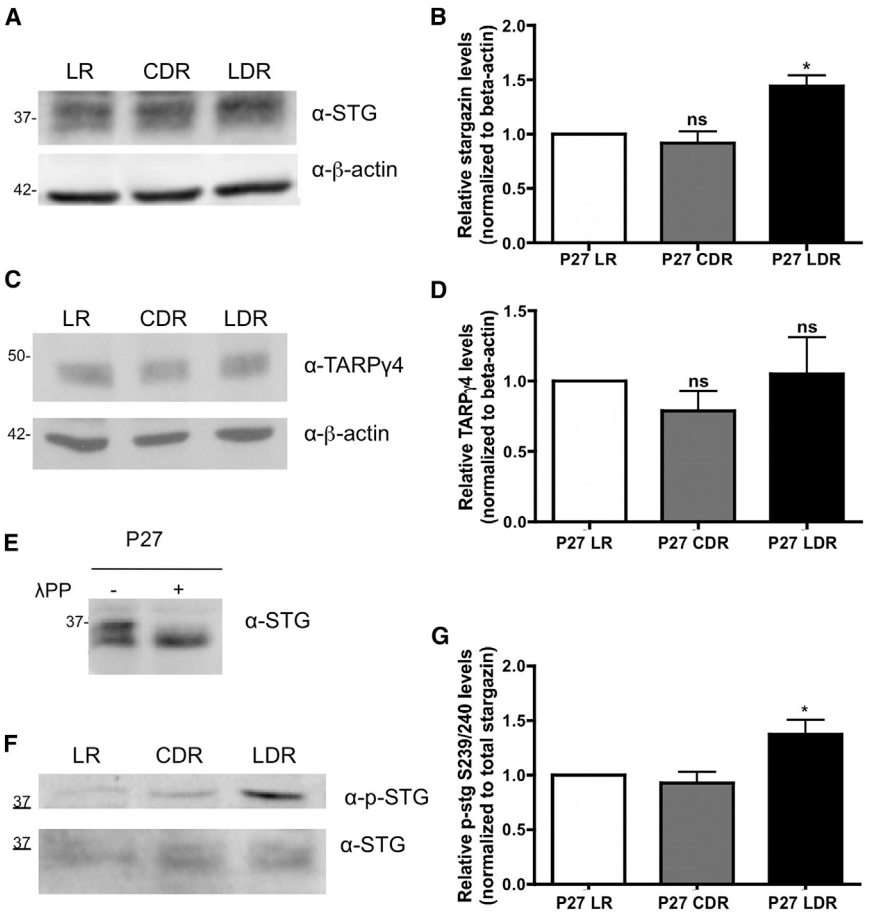

Figure 3. Visual Experience Alters STG Expression and Phosphorylation in the LGN

(A and C) Representative western blot of mouse LGNs (P27) comparing the effects of CDR and LDR on (A) STG and (C) TARPγ4 expression levels.

(B and D) Quantification of average normalized STG (B, n = 4) and TARPγ4 (D, n = 3) levels in CDR and LDR. Data are presented as mean ± SEM.

(E) Effects of lambda-phosphatase on STG mobility in P27 LGN.

(F and G) Comparison of STG phosphorylation at S239/240 in the LGN of LR, CDR, and LDR P27 mice (n = 3; ANOVA, Dunnett's test, *$p < 0.05$ for all the panels in this figure).

In (B), (D), and (G), data are presented as mean ± SEM. See also Figure S3.

STG with PSD-95 (Tomita et al., 2005). STG commonly migrates as a doublet in denaturing SDS-PAGE conditions, and this correlates with the phosphorylation state of the protein (see Figure S3A and Tomita et al., 2005). Consistent with phosphorylated STG in the LGN, we found that lambda-phosphatase treatment of LGN lysates selectively removed the upper, putatively phosphorylated band of the doublet (Figure 3E). We hypothesized that STG phosphorylation is altered in conditions that trigger experience-dependent plasticity; thus, we analyzed relative levels of STG phosphorylation in LR, CDR, and LDR mice using a phospho-specific antibody to two consecutive serine residues: S239 and S240 (Figure S3B). We found a significant increase in STG phosphorylation in LDR mice compared with LR mice (40% ± 13%, p = 0.015, ANOVA followed by Dunnett's test; Figures 3F and 3G). These findings are consistent with the active regulation of STG phosphorylation by a change in vision in relay neurons of the LGN.

Stargazin Modifies AMPAR EPSCs at the Retinogeniculate Synapse

If STG mediates retinogeniculate synapse remodeling in an experience-dependent manner, we might be able to monitor this process functionally. STG modifies the AMPAR I-V relationship such that there is increased rectification at positive holding potentials. Two distinct roles of STG in AMPAR rectification have been described. In cerebellar neurons from stargazer mice, intracellular retention of the GluA2-containing calcium-impermeable AMPAR (CI-AMPAR) (Tomita et al., 2003) leads to increased synaptic accumulation of inwardly rectifying calcium-permeable AMPAR (CP-AMPAR) channels (Bats et al., 2012; Yamazaki et al., 2010, Hollmann et al., 1991). Because CI-AMPAR presents a linear I-V relationship, one can monitor changes in the composition of AMPAR subunit types at synapses functionally by analyzing the AMPAR rectification index (RI; the ratio between the current amplitude at negative potentials to that at positive potentials). Other studies have also demonstrated that STG attenuates AMPAR polyamine block (Soto et al., 2007), which could account for the differences detected in the rectification of AMPAR in stargazer mice.

We analyzed EPSC rectification properties at the retinogeniculate synapse by recording AMPAR-mediated currents at different voltages in the presence of saturating concentrations of intracellular spermine (100 μM), which produces a voltage-dependent block of CP-AMPARs. We found that at P27, AMPAR-mediated currents were more rectified in stargazer mice (p = 0.002, t test), suggesting an increased contribution of CP-AMPARs (Figures 4A and 4B).

We next asked whether a change in the level of STG in the LGN of LDR mice also altered AMPAR current rectification at the retinogeniculate synapse. We compared the rectification properties of the retinogeniculate AMPAR EPSC in visually manipulated mice (Figures 4C and 4D). Consistent with a role for STG in experience-dependent synapse remodeling, CDR did not affect AMPAR rectification, but LDR reduced the RI (I_{-60mV}/I_{+40mV} [Figure 4D], p = 0.007, ANOVA followed by Bonferroni test, LDR compared with LR). Our results demonstrate that STG is present and functional at the retinogeniculate synapse during the vision-sensitive period.

In the LGN, GluA1 is inserted at the retinogeniculate synapse in a vision-dependent manner (Kielland et al., 2009). To test

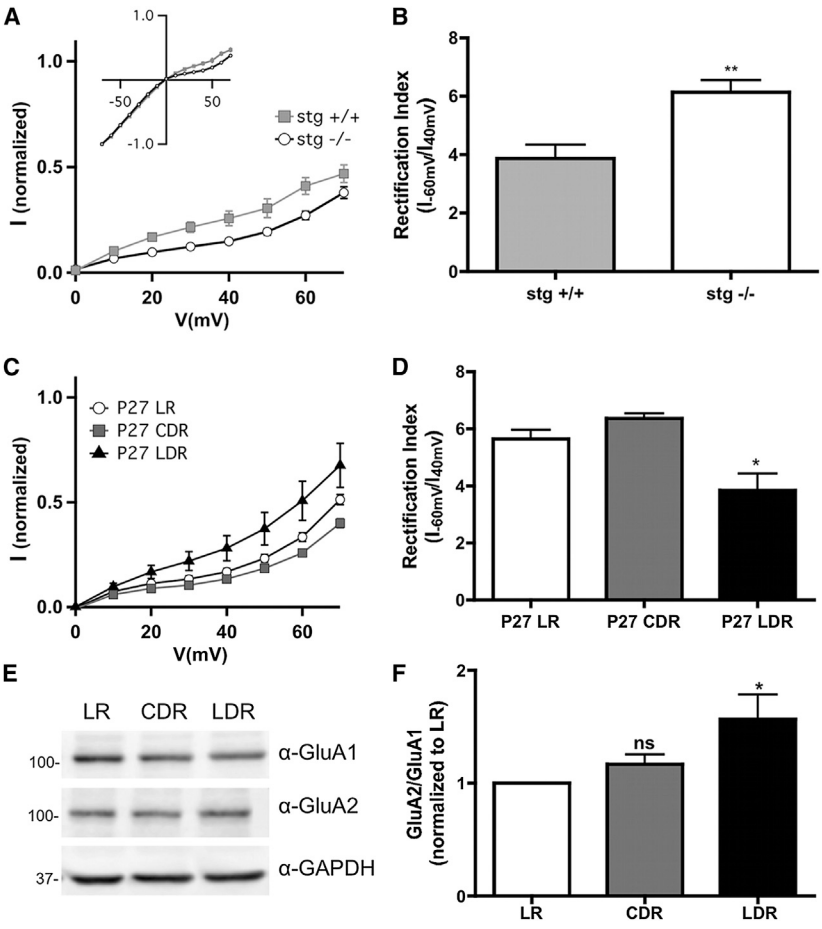

Figure 4. AMPAR Composition in Experience-Dependent Retinogeniculate Plasticity

(A) AMPAR I-Vs normalized to the current amplitude at −70 mV for $stg^{+/+}$ and $stg^{-/-}$ mice. Currents were recorded in the presence of R-CPP and bicuculline in the bath and spermine in the intracellular solution. I-V relationship is shown between 0 and +70 mV, with the full I-V range shown in the inset.

(B) Average RI, $stg^{+/+}$ versus $stg^{-/-}$ (n = 8 $stg^{+/+}$; n = 10 $stg^{-/-}$; p = 0.002, t test).

(C) Normalized I-Vs for C57 mice that experienced different sensory manipulations.

(D) Average RI in visually manipulated mice (n = 4, < 0.05, ANOVA, Bonferroni test, LDR versus LR).

(E) AMPAR subunits GluA1 and GluA2 were analyzed from whole LGN lysates.

(F) The relative abundance of these subunits was plotted as the GluA2/GluA1 ratio (n = 3, ANOVA, Dunnett's test, *p < 0.05, LDR versus LR).

In (B), (D), and (F), data are presented as mean ± SEM.

whether this process might explain the reduction in the AMPAR RI of LDR mice, we examined expression levels of GluA1 and GluA2 subunits in the LGN. Figures 4E and 4F demonstrate a significant increase in the GluA2/GluA1 ratio in the LGN of LDR (p = 0.03, LDR compared with LR, ANOVA followed by Dunnett's test) consistent with higher expression of CI-AMPAR at the retinogeniculate synapse. These results suggest that STG controls AMPAR trafficking and insertion at the retinogeniculate synapse after P20, supporting a model in which STG is required for proper remodeling of the retinogeniculate synapse during the vision-sensitive period.

Stargazin Mediates Synaptic Scaling

Given that synaptic remodeling in the retinogeniculate synapse is triggered by a change in visual activity (Hooks and Chen, 2006) and that LDR increases the maximum AMPAR-evoked currents, we hypothesized that homeostatic adaptation in response to a lack of visual experience occurs in LDR. Further testing of whether STG mediates experience-dependent homeostatic plasticity in vivo was hampered by the fact that the retinogeniculate synapse is part of a larger thalamic circuit in which other connections have been shown to be dependent on STG (Lacey et al., 2012; Menuz and Nicoll, 2008). It was difficult to assess homeostatic responses at one synapse without considering changes at other synapses in the circuit. For this reason, we turned to a simpler culture system in which STG expression could be manipulated in neurons that are innervated by WT inputs. We chose the cortical culture system because it is an established model for studying homeostatic plasticity and, in particular, synaptic scaling. Synaptic scaling is a form of homeostatic plasticity in which neurons adjust their synaptic strength by changing AMPAR content at excitatory synapses in order to maintain stable neuronal output during alterations in network activity (Turrigiano, 2008).

We treated low-density cortical neurons for 48 hr with the voltage-gated Na^+ channel blocker tetrodotoxin (TTX, 1 μM) to block action potential generation, and quantified the surface AMPAR content by incubating live neurons with an antibody specific to the N terminus of the GluA1 subunit (Figure 5A). As previously described (Wierenga et al., 2005), TTX treatment significantly increased the total surface GluA1 cluster fluorescence intensity, area, and number in cortical neurons (p < 0.0001 significantly different from CTR, t test; Figure 5B). Synaptic GluA1 (defined as GluA1 puncta that colocalized with an excitatory postsynaptic marker, PSD95) was also quantified. Chronic treatment with TTX also increased the intensity (p = 0.0007, t test), area (p = 0.0002, t test), and number (p = 0.009, t test) of synaptic GluA1 clusters (Figure 5B). To confirm that the scaling of GluA1 synaptic accumulation was multiplicative (a defining characteristic of synaptic scaling), we plotted ranked control GluA1 synaptic cluster intensities against ranked TTX GluA1 synaptic cluster intensities. The data were well fit by a linear function with a slope of 2.6 (Figure 5C1), which is a multiplicative factor similar to that reported in the initial description of synaptic scaling (Turrigiano et al., 1998). The cumulative distribution of the data acquired from TTX-incubated neurons scaled by this multiplicative factor is almost completely superimposable over the distribution of data from control neurons (Figure 5C2).

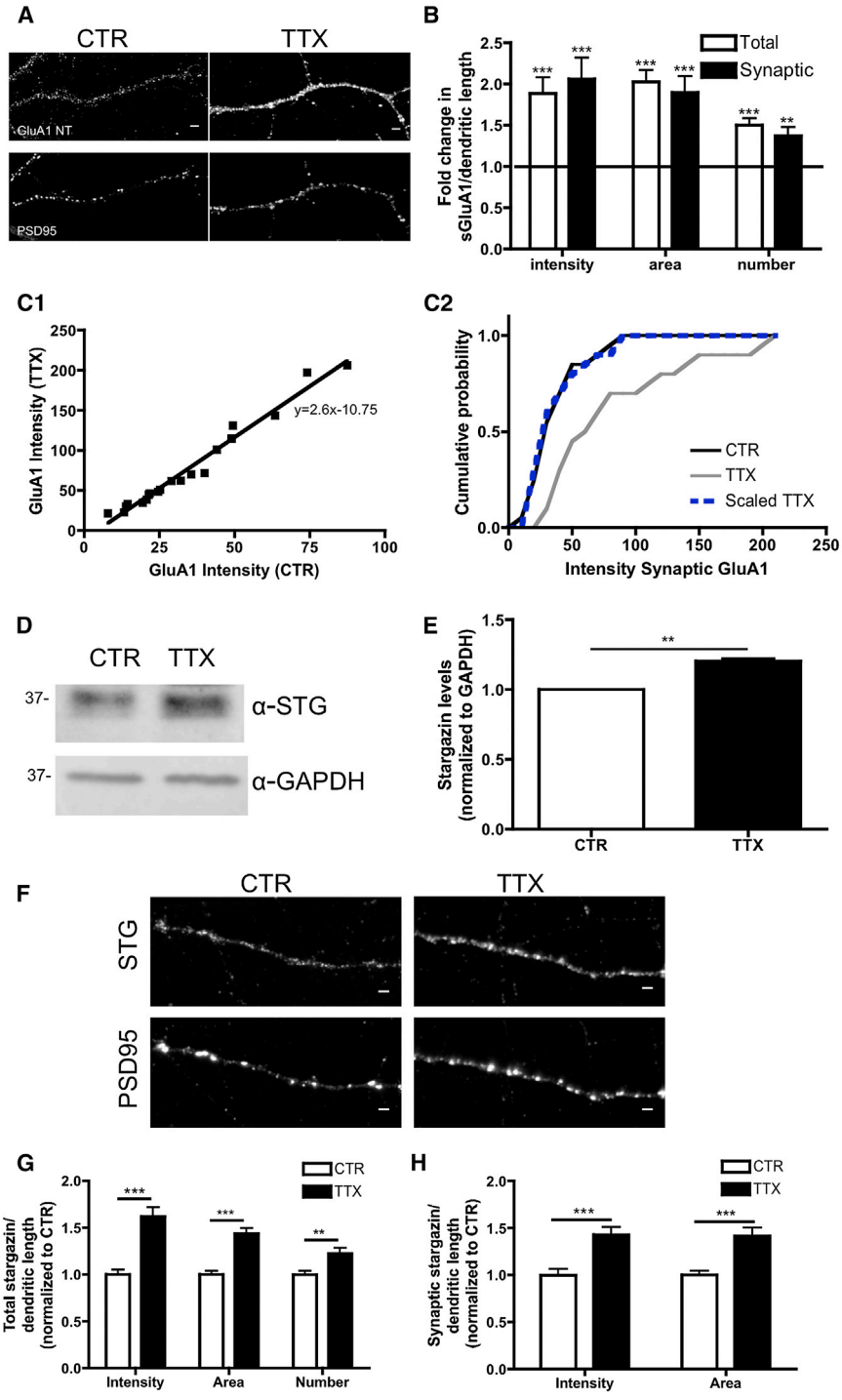

Figure 5. STG Is Increased in Cortical Neurons by TTX-Induced Synaptic Scaling

(A) Representative examples of surface GluA1 (top) and PSD95 (bottom) labeling.

(B) Both total and synaptic surface GluA1 levels were significantly increased by TTX incubation (n = 30 cells each condition, t test,***p < 0.0001 **p < 0.001 compared with CTR).

(C1) Ranked CTR intensities were plotted against ranked TTX intensities and the best-fit function was determined.

(C2) Cumulative distributions of CTR (black) and TTX (gray) synaptic surface GluA1 intensities. The original TTX distribution was transformed by the best-fit equation and plotted (blue dashed line).

(D) Cortical neuron whole-cell lysates were probed with STG and GAPDH antibodies.

(E) Average total STG levels increased by 20.3% ± 2% of control after TTX incubation (n = 3, t test, p = 0.009 versus CTR).

(F) Representative examples of STG (top) and PSD95 (bottom) labeling in CTR vs. TTX-treated neurons.

(G) TTX treatment increased the total STG puncta.

(H) Synaptic STG puncta PSD95, colocalized with PSD95, were increased upon TTX treatment (intensity, area, and number; n = 30 cells for each condition; t test, ***p < 0.0001 vs. CTR).

In (B), (E), (G), and (H), data are presented as mean ± SEM.

These results were consistent with previous reports of TTX-induced global synaptic upscaling, and demonstrated that we could detect synaptic scaling by quantifying synaptic surface GluA1 by immunocytochemistry in low-density cortical neurons.

We next analyzed STG expression in TTX-stimulated cortical neurons and found a significant increase in total STG levels corresponding to homeostatic upregulation of AMPAR (Figures 5D and 5E; p < 0.01, t test). We also analyzed the localization and accumulation of endogenous STG along dendrites by immunofluorescence (Figure 5F). Chronic blockade of neuronal activity with TTX resulted in an accumulation of STG along dendrites, as quantified by an increase in the intensity (p < 0.0001, t test), area (p < 0.0001, t test), and number (p = 0.003, t test) of STG clusters (Figure 5G). Moreover, TTX stimulation increased the intensity (p = 0.0003, t test) and area (p = 0.0002, t test) of STG clusters at synaptic sites (Figure 5H), suggesting a role for STG in AMPAR trafficking during synaptic scaling.

Stargazin Is Essential for Synaptic Scaling

To test whether STG is required for synaptic scaling, we knocked down STG in sparse cultured cortical neurons using a small hairpin RNA (shRNA) sequence against STG mRNA in the pLentiLox3.7(CMV)EGFP vector. shRNA#4 efficiently decreased the intensity of STG immunolabeling to 32.2% ± 3% of endogenous levels (Figures 6B and 6D; p < 0.0001, t test). To investigate the effect of STG knockdown on synaptic scaling, we treated cultured cortical neurons transfected with control shRNA

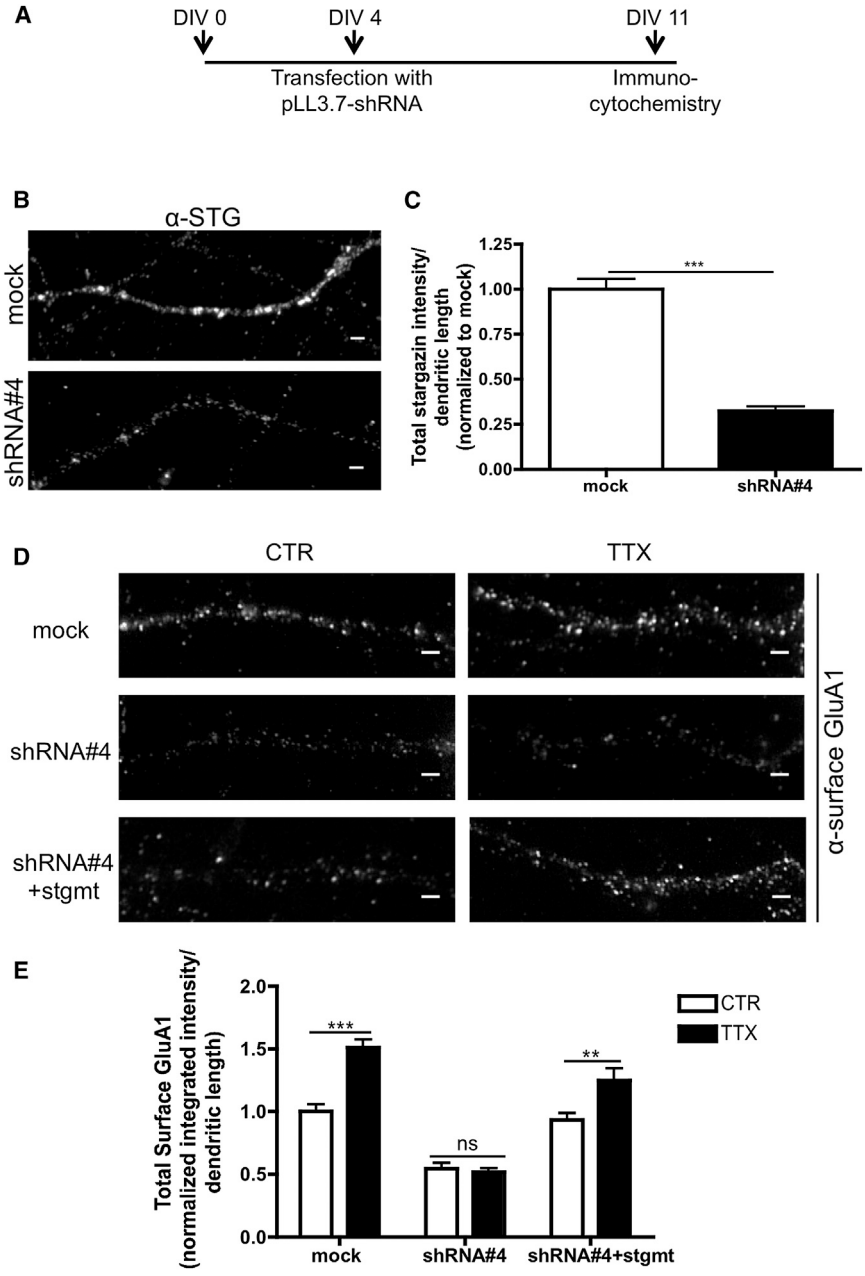

Figure 6. STG Is Essential for Synaptic Scaling

(A) Cortical neurons were transfected with pLL-mock or pLL-shRNA#4 and the total levels of STG were analyzed by immunocytochemistry after 7 days of transfection.

(B and C) Representative images of STG distribution in transfected DIV11 cortical neurons (B) and quantification of the total intensity of STG puncta (C) demonstrate efficient knockdown of the protein by shRNA#4 (32.2% ± 3% of mock, n = 27 cells each condition, p = 0.001, t test).

(D and E) Quantification of surface GluA1 immunocytochemistry comparing the total surface intensity of GluA1 clusters. A normal increase in GluA1 intensity in response to TTX treatment was blocked in neurons transfected with shRNA#4, but not in neurons transfected with shRNA#4 and a STG mutant refractory to this shRNA (n = 26 cells each condition, from three independent experiments; $^{**}p < 0.01$; $^{***}p < 0.001$, ANOVA, Bonferroni test, TTX compared with CTR).

In (C) and (E), data are presented as mean ± SEM.

(mock) or STG shRNA#4 with TTX for 48 hr, and live stained the cultures for cell-surface GluA1 (Figure 6D). In control conditions, STG knockdown caused a 48.4% ± 5% decrease in total surface GluA1 levels (Figure 6E). TTX treatment increased the cell-surface GluA1 in mock-transfected cells ($p < 0.001$, ANOVA followed by the Bonferroni test), but not in cells expressing shRNA#4 (Figure 6E). Importantly, synaptic scaling could be restored by the expression of an shRNA-resistant form of STG (Figure 6E; $p < 0.01$, ANOVA followed by the Bonferroni test). These results demonstrate that STG is essential for synaptic scaling.

Stargazin Phosphorylation Is Required for Synaptic Scaling

CaMKII and PKC can phosphorylate STG at nine serine residues of its intracellular C-terminal tail (Tomita et al., 2005). STG phosphorylation has been implicated in Hebbian forms of synaptic plasticity (Tomita et al., 2005) and in the diffusional trapping of AMPAR at synaptic sites due to increased interaction with PSD95 (Opazo et al., 2010). We found that prolonged inactivity induced by TTX treatment significantly increased activation of PKC (Figures S4A and S4B) and phosphorylation of CaMKIIβ, but not of CaMKIIα (Figures S4C and S4D), consistent with previous reports implicating this isoform in synaptic scaling (Groth et al., 2011; Thiagarajan et al., 2002). To test whether STG phosphorylation was affected by TTX treatment, we looked at the phosphorylation of three serines (S228 and S239/240) using phospho-specific antibodies. Indeed, chronic activity blockade significantly increased STG phosphorylation at S239/240 ($p = 0.005$ CTR versus 48 hr, t test) and S228 ($p = 0.03$ CTR versus 48 hr, t test; Figures 7A and 7B). Interestingly, S239/240 phosphorylation increased within a few hours after TTX application, whereas the increase in S228 phosphorylation could only be detected 48 hr after TTX treatment. To further test whether STG phosphorylation mediates synaptic scaling, we cotransfected cortical neurons with GFP together with either WT STG or mutant forms of STG in which the nine serine phosphorylation sites were genetically altered (Figure 7C). The nine serine residues are mutated to alanine in the phospho-dead

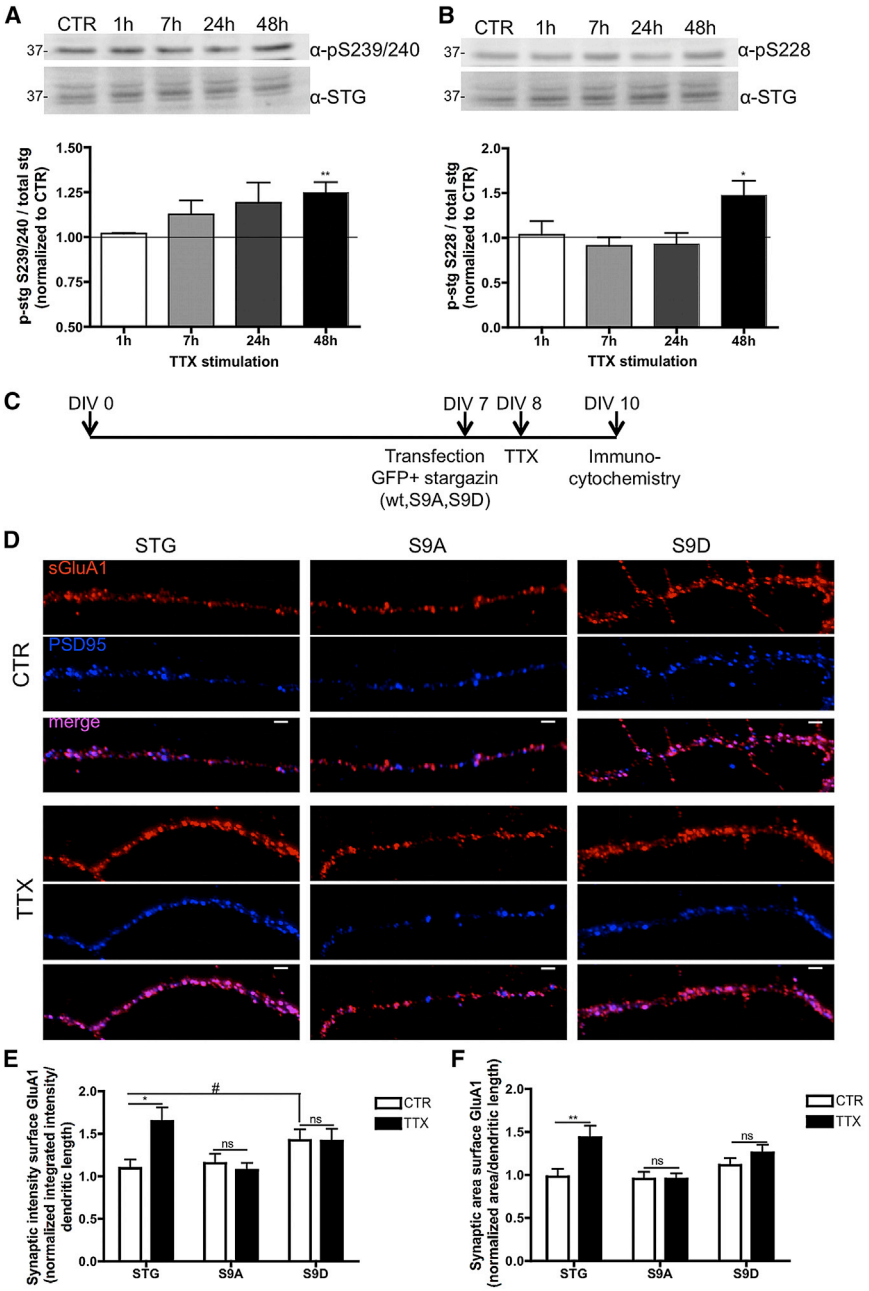

Figure 7. STG Phosphorylation Is Required for Synaptic Scaling

(A) Changes in the phosphorylation of STG after TTX treatment for 1–48 hr. STG phosphorylation at S239/240 increased after 7 hr of activity blockade and was significantly increased after 48 hr of TTX stimulation (n = 4 independent preparations, increase by 24.7% ± 5.8% compared with CTR, p = 0.005, t test).

(B) STG phosphorylation at S228 was significantly increased after 48 hr of activity blockade (n = 4 independent preparations, increase by 47.4% ± 16% compared with CTR, p = 0.031, t test).

(C) Cortical neurons were transfected with WT STG, phospho-dead STG (S9A), or phospho-mimetic STG (S9D) along with GFP and stimulated with TTX.

(D) Surface GluA1 (red) and PSD95 (blue) were analyzed by immunocytochemistry.

(E and F) Activity blockade induced an increase in synaptic surface GluA1 intensity and area in WT STG-transfected neurons, but overexpression of S9A or S9D mutant forms of STG blocked TTX-induced GluA1 accumulation at the surface and synaptic sites. Red, surface GluA1; blue, PSD95; magenta, surface GluA1 colocalized with PSD95. n = 26 cells each condition. **p < 0.01, *p < 0.05, significantly different from CTR; #p < 0.05, S9D CTR significantly different from STG CTR; two-way ANOVA, Bonferroni test.

In (A) and (B), bottom, and (E) and (F), data are presented as mean ± SEM. See also Figures S4 and S5.

mutant of STG (S9A) to mimic the dephosphorylated protein, or replaced by aspartate residues in the phospho-mimetic mutant of STG (S9D) to mimic the fully phosphorylated protein (Tomita et al., 2005). Consistent with previous studies, overexpression of WT STG or S9A did not affect the baseline levels of surface or synaptic GluA1 (Figure 7E), whereas overexpression of S9D increased the baseline levels of AMPAR at the surface of cortical neurons. If the regulation of STG phosphorylation is required for a TTX-induced increase in surface GluA1 expression, we would expect to disrupt synaptic scaling when overexpressing STG mutants. Indeed, overexpression of the STG phospho-dead mutant blocked AMPAR accumulation at synapses in response to TTX (Figure 7E), indicating that STG phosphorylation is required for synaptic scaling. Moreover, overexpression of the phospho-mimetic mutant S9D occluded TTX-induced synaptic scaling (Figure 7E). Altogether, these results strongly support the conclusion that STG phosphorylation is essential for the scaling of glutamatergic synapses.

The insertion of different subunits of AMPARs during homeostatic plasticity remains controversial and seems to be dependent on the model system or stimuli used to induce synaptic scaling (reviewed by Lee, 2012). To look at different AMPAR subunits at the surface of cortical neurons after synaptic scaling induction, we biotinylated and isolated cell-surface proteins. Consistent with Figure 7, we observed an increase in GluA1 surface accumulation upon chronic inactivity, but GluA2 subunit surface accumulation increased further, resulting in a 21.2% ± 2.8% increase in total GluA2/GluA1 ratio (p = 0.017, t test) and a 25.7% ± 2.3% increase in GluA2/GluA1 surface expression (Figure S5; p = 0.008, t test). This may be due to an accumulation of both GluA1-GluA2 and GluA2-GluA3 heteromers at the surface of cortical neurons after 48 hr of inactivity. The overexpression of STG phospho-mutants differentially affected surface insertion

of the GluA1 and GluA2 subunits of AMPAR during chronic inactivity (Figures S5C and S5D). We confirmed the results from our single-cell analysis (Figures 7E and 7F), which showed that expression of STG phospho-mutants blocked a TTX-induced GluA1 increase at the surface of neurons (Figure S5E). Interestingly, GluA2 subunit insertion was differentially affected by the expression of the two STG phospho mutants (Figure S5F), raising the interesting possibility that the phosphorylation of STG may influence the interaction of GluA2-containing receptors with other interactors that have been implicated in scaling up, such as PICK1 (Anggono et al., 2011).

DISCUSSION

In this study, we uncover a role for STG in experience-dependent plasticity. We show that LDR, a manipulation that elicits a homeostatic-like remodeling of the retinogeniculate connection, regulates the STG phosphorylation state and AMPAR composition. Phosphorylation of STG is necessary for scaling up of synaptic strength in TTX-treated cortical neurons. Common features were found between chronic inactivity induced by TTX in cortical neurons and the retinogeniculate synapse properties after LDR in mice, with a significant upregulation of STG and GluA2-containing AMPAR in both conditions. These findings suggest that phosphorylation of STG can mediate synaptic plasticity and remodeling during critical periods of sensory circuit development.

Phosphorylation of Stargazin Regulates Synaptic Scaling

Previous studies have identified STG as a critical mediator of long-term synaptic plasticity (LTP and LTD). STG phosphorylation at nine serine residues is regulated by neuronal activity through the activation of PKC and CaMKII (Tomita et al., 2005). Phosphorylation of the TARP decreases STG-lipid interactions and enhances PSD95-STG interaction (Bats et al., 2007; Schnell et al., 2002; Sumioka et al., 2010), resulting in AMPAR immobilization at the PSD (Opazo et al., 2010) and synaptic strengthening. Through the phosphorylation and dephosphorylation of STG, synapse-specific LTP and LTD can be regulated (Tomita et al., 2005). Here, we demonstrate that in addition to STG's role in Hebbian-like plasticity, STG phosphorylation is essential for synaptic upscaling in response to chronic activity blockade. In cortical cultures, we found that STG phosphorylation was increased by chronic inactivity. In addition, overexpression of STG phospho mutants led to complete blockade or occlusion of synaptic scaling. It is important to note that expression of the phospho-dead (S9A) mutant of STG did not affect AMPAR accumulation at synapses, arguing against the trivial explanation that the results are secondary to a disruption of AMPAR trafficking into the synapse. Instead, our data show that phosphorylation of STG is essential for synaptic scaling in response to chronic activity blockade.

How STG phosphorylation differentiates between Hebbian and homeostatic plasticity is still unclear. Recent studies have suggested that the two forms of plasticity can interact. Conditions that silence neuronal activity can also enhance LTP (Arendt et al., 2013). Moreover, experience-dependent homeostatic adaptation in the visual cortex can be reversed through Hebbian plasticity mechanisms (Desai et al., 2002; Goel et al., 2006; He et al., 2007). Although both PKC and CaMKII play a role in synaptic scaling and LTP (Lisman et al., 2012; Malinow et al., 1988; Nicoll and Roche, 2013), signaling upstream of these enzymes or subcellular localization of activated PKC/CaMKII could be distinct. Other possibilities include a site-specific phosphorylation code and/or a temporal sequence in serine phosphorylation. The latter is an attractive model that is supported by our findings that the time course for phosphorylation of S239/S249 and S228 in STG differs in response to chronic inactivity, and is consistent with the finding that different phosphorylation sites regulate the binding of STG to other proteins (Matsuda et al., 2013). In the future, it will be interesting to test whether phosphorylation of specific serine residues distinguishes between the two fundamentally different forms of synaptic plasticity.

Regulation of Stargazin In Vivo by Visual Experience

Classic in vitro studies of STG have provided great insight into how activity regulates AMPAR trafficking (Jackson and Nicoll, 2011). How physiological stimuli regulate STG in vivo is less clear. Here, we turned to the visual system, where developmental refinement of synaptic circuits is driven by both spontaneous and experience-dependent plasticity (Hong and Chen, 2011). We show that sensory experience can regulate STG expression and phosphorylation. Our data demonstrate that during the developmental period driven by spontaneous activity, STG is expressed in the LGN, and loss of STG disrupts the AMPAR/NMDAR ratios at the retinogeniculate synapse. STG expression levels increase during development in both normally reared and CDR mice. However, visually depriving mice during the experience-sensitive critical period further increases both the STG levels and the phosphorylation of serine residues present at the C-terminal tail of STG. Consistent with a role for STG in this late phase of synapse remodeling, the developmental convergence of afferent inputs is not disrupted until after P21 in *stg*$^{-/-}$ mice. During this phase, the reduced synaptic strength and apparent increase in afferent inputs is likely a result of high mobility of AMPAR in and out of synaptic sites in the absence of STG. Our results suggest that during the normal light experience, STG phosphorylation is responsible for stabilization of the refined retinogeniculate connection.

Remarkably, the regulation of STG by visual experience occurred during a limited window of time. Shifting the onset of dark rearing by 5 days (DR from P25 to P32), a manipulation that does not induce remodeling at the retinogeniculate synapse (delayed DR; Hooks and Chen, 2008), also did not alter STG expression levels (Figure S6). Moreover, the regulation of STG by sensory activity cannot be generalized to all TARPS, given that TARPγ4 was not sensitive to visual manipulations. Thus, STG is a TARP that specifically mediates experience-dependent synaptic plasticity at this thalamic synapse. Based on our findings, we propose that different phases of retinogeniculate synapse maturation depend on distinct molecular pathways, with the phosphorylation of STG mediating the experience-dependent plasticity phase of remodeling.

AMPAR Composition in Experience-Dependent Synapse Remodeling

Our results show that STG regulates AMPAR rectification at the retinogeniculate synapse during the late phase of development. Loss of STG increases AMPAR rectification, whereas increased expression of STG in response to LDR leads to a more linear I-V. Two mechanisms underlying STG's role in rectification have been described: one involves trafficking of specific AMPAR subunits into the synapse, and the other entails reducing the CP-AMPAR affinity to intracellular polyamines (Soto et al., 2007). At the retinogeniculate synapse, we believe that STG is involved in the trafficking of more GluA2-containing AMPAR during LDR, for several reasons. First, we found an increase in the GluA2/GluA1 ratio in the immunoblots of LGN of LDR mice compared with LR mice, consistent with increased expression of GluA2-containing AMPAR at relay neurons. In addition, we detected intracellular accumulation of GluA2 subunit in LGN of stargazer mice by deglycosylation analysis (data not shown), as previously shown for the cerebellum of stargazer mice (Tomita et al., 2003). Finally, the change in the GluA2/GluA1 ratio in LDR is consistent with a previous report by Kielland et al. (2009), who found that whereas relay neurons in the visual thalamus receive glutamatergic inputs from both the retina and the cortex, GluA1 subunits are preferentially inserted into retinal synapses in response to visual stimulation. Interestingly, visual deprivation from birth (CDR) does not alter the I-V relationship in the same manner as LDR, supporting our hypothesis that turnover of AMPAR subunits occurs in response to changes in vision during a discrete period of time.

Based on our studies, we cannot distinguish whether STG preferentially traffics GluA2 over GluA1, as suggested by some reports (Tomita et al., 2003), or whether the composition of AMPAR is determined by the intracellular abundance of the subunit (Chen et al., 2000). It is also unclear whether the specific AMPAR subunit class is important for homeostatic plasticity at the retinogeniculate synapse. Regardless, we were able to monitor the effect of STG on AMPAR trafficking into the retinogeniculate synapse during the vision-sensitive period.

Homeostatic Plasticity and the Visual System

Homeostatic plasticity in response to changes in activity plays an important role in the development of the visual system (Maffei and Turrigiano, 2008). In the visual cortex, this form of plasticity occurs in response to visual deprivation during specific windows of development (Desai et al., 2002) and plays a role in ocular dominance plasticity (Kaneko et al., 2008; Mrsic-Flogel et al., 2007). Around the time of eye opening, monocular deprivation can increase spontaneous corticothalamic activity (Krahe and Guido, 2011). In the superior colliculus, homeostatic mechanisms contribute to the conservation of total retinocollicular input in response to disruption of spontaneous retinal wave activity (Chandrasekaran et al., 2005, 2007).

Consistent with the above-cited studies, the synaptic response to LDR has many features of homeostatic plasticity. Synaptic remodeling is elicited by a change in vision—CDR does not exhibit plasticity even though sensory experience is the same as LDR between P20 and P34. Moreover, the recruitment in LDR of more afferent inputs offsets the reduction in single-fiber strength and leads to an increase in maximal currents. Here, we present evidence that LDR-elicited retinogeniculate plasticity shares molecular pathways with in vitro synaptic scaling, showing that STG is regulated by vision in the LGN and that disrupting STG function interferes with experience-dependent remodeling of the retinogeniculate synapse. Based on these results, we propose that LDR elicits a homeostatic upregulation of AMPAR in the retinogeniculate synapse. Increased STG expression and phosphorylation mediate the insertion of AMPAR into previously silent or weak synaptic sites throughout the relay neuron, resulting in a change in the number of afferent RGC inputs. Taken together, our data show an important role for STG phosphorylation in synaptic upscaling and sensory-dependent synapse remodeling.

EXPERIMENTAL PROCEDURES

Animals

stg+/+ and *stg*−/− littermates and C57BL/6 mice were used in this study. For dark-rearing experiments, mothers with P0 or P20 litters were placed for 7 days in a light-tight container in which temperature, humidity, and luminance were continually monitored (Hooks and Chen, 2006). Control (normally light-reared, LR) animals were raised under a 12 hr light/dark cycle. For cortical neurons cultures, pregnant Wistar rats were used. All the procedures were reviewed and approved by the IACUC at Children's Hospital, Boston, or by the Portuguese National Authority for Animal Health (DGAV).

Electrophysiology

Acute LGN brain slices and the electrophysiological methods used to study development of the retinogeniculate synapse have been described previously (Chen and Regehr, 2000; Hooks and Chen, 2006, 2008). Peak single-fiber AMPAR EPSC amplitudes were obtained from minimal stimulation (Chen and Regehr, 2000). Single-fiber measurements included a second input from a given cell if it was recruited during an incremental increase in stimulus intensity (0.25 μA) and was clearly resolvable (5-fold greater in amplitude) from the first input. For details, see Supplemental Experimental Procedures.

Immunocytochemistry

Low-density rat cortical neurons were fixed in 4% paraformaldehyde and incubated with the antibodies stargazin (ab64237; Abcam), PSD95 (MA1-045; Thermo Scientific), and Map2 (ab5392; Abcam) as previously described (Santos et al., 2012). For cell-surface staining of GluA1, anti-GluA1 N-terminal antibody was added to neurons for 10 min at room temperature. The neurons were washed and then fixed as described above. For details, see Supplemental Experimental Procedures.

Western Blot

High-density rat cortical neurons were lysed with TEEN buffer (25 mM Tris-Cl, pH 7.4, 1 mM EDTA, 1 mM EGTA, 150 mM NaCl, and 1% Triton X-100) supplemented with protease and phosphatase inhibitors. The following Merck Millipore antibodies were used: anti-stargazin (AB9876), anti-phospho stargazin (Ser239/Ser240; AB3713), anti-phospho stargazin (Ser228; AB15435), anti-GluA1 (AB1504), and anti-GluA2 (MAB397).

Statistical Analysis

The normality of current amplitude distributions was tested by comparison with a theoretical normal distribution using a Kolmogorov-Smirnov test. Statistical significance was tested using Kruskal-Wallis or Mann-Whitney tests because the maximal current and single-fiber current values were typically not normally distributed. Biochemical and immunocytochemical data are presented as mean ± SEM of at least three different experiments, performed in independent preparations. Statistical analysis of the results was performed using either paired Student's t test or one-way or two-way ANOVA followed

by either Dunnett's or Bonferroni post test (n.s., nonsignificant, ***$p < 0.001$, **$p < 0.01$, *$p < 0.05$).

SUPPLEMENTAL INFORMATION

Supplemental Information includes Supplemental Experimental Procedures and six figures and can be found with this article online at http://dx.doi.org/10.1016/j.celrep.2014.04.054.

ACKNOWLEDGMENTS

We thank the Greenberg lab for assistance in designing the shRNA#4, Dr. S. Tomita (Yale University) for the kind gift of STG phosphomutant constructs, and Dr. Andrew Irving (University of Dundee) for the GluA1 N terminus antibody. We are grateful to C.B. Duarte, A. Thompson, J. Hauser, J. Leffler, M.E. Greenberg, and T. Schwarz for critical readings of the manuscript. We also thank E. Carvalho for assistance in the preparation of cultured neurons. S.R.L. was supported by FCT, Portugal. This work was supported by grants from FCT and FEDER, Portugal (PEst-C/SAU/LA0001/2013-2014, PTDC/SAU-NEU/099440/2008, and PTDC/NEU-NCM/0750/2012 to A.L.C.), and the NIH (F31 NS048630 to B.M.H., and EY013613 and HD018655 to C.C.).

Received: August 28, 2013
Revised: January 19, 2014
Accepted: April 24, 2014
Published: May 29, 2014

REFERENCES

Anggono, V., Clem, R.L., and Huganir, R.L. (2011). PICK1 loss of function occludes homeostatic synaptic scaling. J. Neurosci. *31*, 2188–2196.

Arendt, K.L., Sarti, F., and Chen, L. (2013). Chronic inactivation of a neural circuit enhances LTP by inducing silent synapse formation. J. Neurosci. *33*, 2087–2096.

Bats, C., Groc, L., and Choquet, D. (2007). The interaction between Stargazin and PSD-95 regulates AMPA receptor surface trafficking. Neuron *53*, 719–734.

Bats, C., Soto, D., Studniarczyk, D., Farrant, M., and Cull-Candy, S.G. (2012). Channel properties reveal differential expression of TARPed and TARPless AMPARs in stargazer neurons. Nat. Neurosci. *15*, 853–861.

Blackman, M.P., Djukic, B., Nelson, S.B., and Turrigiano, G.G. (2012). A critical and cell-autonomous role for MeCP2 in synaptic scaling up. J. Neurosci. *32*, 13529–13536.

Burgess, D.L., and Noebels, J.L. (1999). Single gene defects in mice: the role of voltage-dependent calcium channels in absence models. Epilepsy Res. *36*, 111–122.

Butts, D.A., Kanold, P.O., and Shatz, C.J. (2007). A burst-based "Hebbian" learning rule at retinogeniculate synapses links retinal waves to activity-dependent refinement. PLoS Biol. *5*, e61.

Chandrasekaran, A.R., Plas, D.T., Gonzalez, E., and Crair, M.C. (2005). Evidence for an instructive role of retinal activity in retinotopic map refinement in the superior colliculus of the mouse. J. Neurosci. *25*, 6929–6938.

Chandrasekaran, A.R., Shah, R.D., and Crair, M.C. (2007). Developmental homeostasis of mouse retinocollicular synapses. J. Neurosci. *27*, 1746–1755.

Chen, C., and Regehr, W.G. (2000). Developmental remodeling of the retinogeniculate synapse. Neuron *28*, 955–966.

Chen, L., Chetkovich, D.M., Petralia, R.S., Sweeney, N.T., Kawasaki, Y., Wenthold, R.J., Bredt, D.S., and Nicoll, R.A. (2000). Stargazin regulates synaptic targeting of AMPA receptors by two distinct mechanisms. Nature *408*, 936–943.

Desai, N.S., Cudmore, R.H., Nelson, S.B., and Turrigiano, G.G. (2002). Critical periods for experience-dependent synaptic scaling in visual cortex. Nat. Neurosci. *5*, 783–789.

Fukaya, M., Yamazaki, M., Sakimura, K., and Watanabe, M. (2005). Spatial diversity in gene expression for VDCCgamma subunit family in developing and adult mouse brains. Neurosci. Res. *53*, 376–383.

Goel, A., Jiang, B., Xu, L.W., Song, L., Kirkwood, A., and Lee, H.K. (2006). Cross-modal regulation of synaptic AMPA receptors in primary sensory cortices by visual experience. Nat. Neurosci. *9*, 1001–1003.

Groth, R.D., Lindskog, M., Thiagarajan, T.C., Li, L., and Tsien, R.W. (2011). Beta Ca2+/CaM-dependent kinase type II triggers upregulation of GluA1 to coordinate adaptation to synaptic inactivity in hippocampal neurons. Proc. Natl. Acad. Sci. USA *108*, 828–833.

He, H.Y., Ray, B., Dennis, K., and Quinlan, E.M. (2007). Experience-dependent recovery of vision following chronic deprivation amblyopia. Nat. Neurosci. *10*, 1134–1136.

Hollmann, M., Hartley, M., and Heinemann, S. (1991). Ca2+ permeability of KA-AMPA—gated glutamate receptor channels depends on subunit composition. Science *252*, 851–853.

Hong, Y.K., and Chen, C. (2011). Wiring and rewiring of the retinogeniculate synapse. Curr. Opin. Neurobiol. *21*, 228–237.

Hooks, B.M., and Chen, C. (2006). Distinct roles for spontaneous and visual activity in remodeling of the retinogeniculate synapse. Neuron *52*, 281–291.

Hooks, B.M., and Chen, C. (2008). Vision triggers an experience-dependent sensitive period at the retinogeniculate synapse. J. Neurosci. *28*, 4807–4817.

Jackson, A.C., and Nicoll, R.A. (2011). The expanding social network of ionotropic glutamate receptors: TARPs and other transmembrane auxiliary subunits. Neuron *70*, 178–199.

Kaneko, M., Stellwagen, D., Malenka, R.C., and Stryker, M.P. (2008). Tumor necrosis factor-alpha mediates one component of competitive, experience-dependent plasticity in developing visual cortex. Neuron *58*, 673–680.

Kielland, A., Bochorishvili, G., Corson, J., Zhang, L., Rosin, D.L., Heggelund, P., and Zhu, J.J. (2009). Activity patterns govern synapse-specific AMPA receptor trafficking between deliverable and synaptic pools. Neuron *62*, 84–101.

Krahe, T.E., and Guido, W. (2011). Homeostatic plasticity in the visual thalamus by monocular deprivation. J. Neurosci. *31*, 6842–6849.

Lacey, C.J., Bryant, A., Brill, J., and Huguenard, J.R. (2012). Enhanced NMDA receptor-dependent thalamic excitation and network oscillations in stargazer mice. J. Neurosci. *32*, 11067–11081.

Lee, H.K. (2012). Ca-permeable AMPA receptors in homeostatic synaptic plasticity. Front. Mol. Neurosci. *5*, 17.

Letts, V.A., Felix, R., Biddlecome, G.H., Arikkath, J., Mahaffey, C.L., Valenzuela, A., Bartlett, F.S., 2nd, Mori, Y., Campbell, K.P., and Frankel, W.N. (1998). The mouse stargazer gene encodes a neuronal Ca2+-channel gamma subunit. Nat. Genet. *19*, 340–347.

Lin, D.J., Kang, E., and Chen, C. (2014). Changes in input strength and number are driven by distinct mechanisms at the retinogeniculate synapse. J. Neurophysiol. http://dx.doi.org/10.1152/jn.00175.2014.

Lisman, J., Yasuda, R., and Raghavachari, S. (2012). Mechanisms of CaMKII action in long-term potentiation. Nat. Rev. Neurosci. *13*, 169–182.

Maffei, A., and Turrigiano, G. (2008). The age of plasticity: developmental regulation of synaptic plasticity in neocortical microcircuits. Prog. Brain Res. *169*, 211–223.

Malinow, R., Madison, D.V., and Tsien, R.W. (1988). Persistent protein kinase activity underlying long-term potentiation. Nature *335*, 820–824.

Matsuda, S., Kakegawa, W., Budisantoso, T., Nomura, T., Kohda, K., and Yuzaki, M. (2013). Stargazin regulates AMPA receptor trafficking through adaptor protein complexes during long-term depression. Nat Commun *4*, 2759.

Menuz, K., and Nicoll, R.A. (2008). Loss of inhibitory neuron AMPA receptors contributes to ataxia and epilepsy in stargazer mice. J. Neurosci. *28*, 10599–10603.

Mrsic-Flogel, T.D., Hofer, S.B., Ohki, K., Reid, R.C., Bonhoeffer, T., and Hübener, M. (2007). Homeostatic regulation of eye-specific responses in visual cortex during ocular dominance plasticity. Neuron *54*, 961–972.

Nicoll, R.A., and Roche, K.W. (2013). Long-term potentiation: peeling the onion. Neuropharmacology *74*, 18–22.

Noutel, J., Hong, Y.K., Leu, B., Kang, E., and Chen, C. (2011). Experience-dependent retinogeniculate synapse remodeling is abnormal in MeCP2-deficient mice. Neuron *70*, 35–42.

Ohara, P.T., Lieberman, A.R., Hunt, S.P., and Wu, J.Y. (1983). Neural elements containing glutamic acid decarboxylase (GAD) in the dorsal lateral geniculate nucleus of the rat; immunohistochemical studies by light and electron microscopy. Neuroscience *8*, 189–211.

Opazo, P., Labrecque, S., Tigaret, C.M., Frouin, A., Wiseman, P.W., De Koninck, P., and Choquet, D. (2010). CaMKII triggers the diffusional trapping of surface AMPARs through phosphorylation of stargazin. Neuron *67*, 239–252.

Payne, H.L. (2008). The role of transmembrane AMPA receptor regulatory proteins (TARPs) in neurotransmission and receptor trafficking (Review). Mol. Membr. Biol. *25*, 353–362.

Qiu, Z., Sylwestrak, E.L., Lieberman, D.N., Zhang, Y., Liu, X.Y., and Ghosh, A. (2012). The Rett syndrome protein MeCP2 regulates synaptic scaling. J. Neurosci. *32*, 989–994.

Santos, S.D., Iuliano, O., Ribeiro, L., Veran, J., Ferreira, J.S., Rio, P., Mulle, C., Duarte, C.B., and Carvalho, A.L. (2012). Contactin-associated protein 1 (Caspr1) regulates the traffic and synaptic content of α-amino-3-hydroxy-5-methyl-4-isoxazolepropionic acid (AMPA)-type glutamate receptors. J. Biol. Chem. *287*, 6868–6877.

Schnell, E., Sizemore, M., Karimzadegan, S., Chen, L., Bredt, D.S., and Nicoll, R.A. (2002). Direct interactions between PSD-95 and stargazin control synaptic AMPA receptor number. Proc. Natl. Acad. Sci. USA *99*, 13902–13907.

Soto, D., Coombs, I.D., Kelly, L., Farrant, M., and Cull-Candy, S.G. (2007). Stargazin attenuates intracellular polyamine block of calcium-permeable AMPA receptors. Nat. Neurosci. *10*, 1260–1267.

Sumioka, A., Yan, D., and Tomita, S. (2010). TARP phosphorylation regulates synaptic AMPA receptors through lipid bilayers. Neuron *66*, 755–767.

Thiagarajan, T.C., Piedras-Renteria, E.S., and Tsien, R.W. (2002). alpha- and betaCaMKII. Inverse regulation by neuronal activity and opposing effects on synaptic strength. Neuron *36*, 1103–1114.

Tomita, S., Chen, L., Kawasaki, Y., Petralia, R.S., Wenthold, R.J., Nicoll, R.A., and Bredt, D.S. (2003). Functional studies and distribution define a family of transmembrane AMPA receptor regulatory proteins. J. Cell Biol. *161*, 805–816.

Tomita, S., Stein, V., Stocker, T.J., Nicoll, R.A., and Bredt, D.S. (2005). Bidirectional synaptic plasticity regulated by phosphorylation of stargazin-like TARPs. Neuron *45*, 269–277.

Turrigiano, G.G. (2008). The self-tuning neuron: synaptic scaling of excitatory synapses. Cell *135*, 422–435.

Turrigiano, G.G., Leslie, K.R., Desai, N.S., Rutherford, L.C., and Nelson, S.B. (1998). Activity-dependent scaling of quantal amplitude in neocortical neurons. Nature *391*, 892–896.

Wierenga, C.J., Ibata, K., and Turrigiano, G.G. (2005). Postsynaptic expression of homeostatic plasticity at neocortical synapses. J. Neurosci. *25*, 2895–2905.

Yamazaki, M., Fukaya, M., Hashimoto, K., Yamasaki, M., Tsujita, M., Itakura, M., Abe, M., Natsume, R., Takahashi, M., Kano, M., et al. (2010). TARPs gamma-2 and gamma-7 are essential for AMPA receptor expression in the cerebellum. Eur. J. Neurosci. *31*, 2204–2220.

Zhong, X., Li, H., and Chang, Q. (2012). MeCP2 phosphorylation is required for modulating synaptic scaling through mGluR5. J. Neurosci. *32*, 12841–12847.

Ziburkus, J., Dilger, E.K., Lo, F.S., and Guido, W. (2009). LTD and LTP at the developing retinogeniculate synapse. J. Neurophysiol. *102*, 3082–3090.